JMEPEG (2010) 19:264–273
DOI: 10.1007/s11665-009-9455-1
©ASM International
1059-9495/$19.00

Investigation into Microstructures of Maraging Steel 250 Weldments and Effect of Post-Weld Heat Treatments

Fawad Tariq, Rasheed Ahmed Baloch, Bilal Ahmed, and Nausheen Naz

(Submitted September 11, 2008; in revised form February 28, 2009)

This study was undertaken to gain a better understanding of microstructures obtained by multipass gas tungsten arc welding in maraging steel grade 250. Metallography and microhardness measurements were carried out on sheet and welded joints in as-welded and post-weld aged conditions. It was found that there was a significant amount of reverted austenite formed on cell boundaries of weld metal after aging at 758-823 K for 3-5 h, and was stable at room temperature. Aging at higher temperatures led to an increase in the continuous network of patchy austenite along the cell boundaries. The reason for the above, in our opinion, is the concentrational heterogeneity which characterizes the microstructure of maraging steel welds. No reverted austenite was observed in as-welded specimens. Solution annealing at 1093 K for 1 h did not completely eliminate the chemical heterogeneity associated with weld structures. However, homogenizing at 1373 K produced homogenous structure that on subsequent aging produces austenite-free lath martensitic structure.

Keywords aging, heat-affected zone, maraging steel, precipitation, reverted austenite

1. Introduction

Aerospace design requirements are making increasing demands for better performance with greater efficiency in the use of high strength structural materials. Because of high strength and toughness combinations achievable in maraging steels, these materials have been understudy for the last four decades. Carbon-free 18Ni maraging steels are the most promising steels that exceed other structural materials but their cost is higher because of high percentage of expensive alloying elements.

These steels are based on low-carbon Fe-Ni system with varying percentages of Co, Mo, Ti, and Al. The most widely used combination is 18% Ni, 8-9% Co, and 3-5% Mo. They derive their superior mechanical properties by two solid-state reactions called MAR-AGING (i.e., martensitic transformation followed by aging). It is well known that the increase in the strength of Ni-Co-Mo maraging steels is caused by precipitation of intermetallic compounds of type $(Fe, Ni)_2Mo$ and Ni_3Mo (at $<5\%$ Mo), Ni_3Mo (at $>5\%$ Mo), and Fe_7Mo (at $>10\%$ Mo) (Ref 1-3). Ribbon-shaped Ni_3Mo is the major precipitate, with the secondary Ni_3Ti being uniformly distributed as spherical particles. Cobalt accelerates the rate of precipitation but does not itself precipitate (Ref 4).

Weldability is one of the most important properties of ultra-high strength steels, especially in Aviation and Space Industry. The unique property of maraging steels of being weldable in solution annealed and aged condition make these steels attractive for fabrication of large structures (Ref 5). Among several welding techniques, gas tungsten arc welding (GTAW) is the most widely employed welding technique for joining large thin-walled pressure vessels and various parts and assemblies due to its high weld quality and reduced cost. However, production of large structures of maraging steels by welding requires a close control of welding parameters and post-weld aging treatment. Since microstructure has a major influence on mechanical properties; it is, therefore, necessary to identify different phases formed during welding and subsequent heat treatments and control them to obtain desired set of properties.

In this paper, effects of multi-pass GTAW and post-weld aging treatments on microstructures and mechanical properties of maraging steel (grade 250) weldments were studied. Tensile tests were carried out on sheet and welded specimens in as-welded and post-weld aged conditions. Metallographic examination and microhardness measurements were carried out on as-welded as well as on post-weld aged specimens. Aging was carried out at 758, 773, 793, and 823 K for 3 and 5 h.

2. Experimental Work

The investigation was conducted on 18 Ni maraging steel (grade 250) that was produced from electric arc furnace, vacuum degassed, and electro-slag remelted. The chemical composition of the maraging steel sheets used in this study is given in Table 1. Hot rolled sheets of 5.5 mm thickness were multipass butt welded by GTAW (DC) using filler wire of composition given in Table 1. The first pass was made without filler wire. Inter-pass temperature was kept below 373 K. X-ray radiography of the welded structures did not show any defects.

Fawad Tariq, Rasheed Ahmed Baloch, Bilal Ahmed, and **Nausheen Naz**, Materials Research and Testing Laboratory, Pakistan Space and Upper Atmosphere Research Commission (SUPARCO), Karachi, Pakistan. Contact e-mail: t_fawad@hotmail.com.

Table 1 Chemical composition (in wt.%) of maraging steel (grade 250) sheet and filler wire

Maraging steel 250	C	Si	Mn	Ni	Co	Mo	Ti	Al	S	P	Fe
Sheet	0.01	0.06	0.03	17.97	7.97	5.03	0.50	0.11	0.008	0.005	Bal.
Filler wire	0.03	0.1	0.1	18.31	8.95	4.94	0.72	0.10	0.010	0.010	Bal.

Table 2 Mechanical properties of maraging steel (grade 250) sheet and welded specimens

Treatment	0.2% Yield strength, MPa	Tensile strength, MPa	% Elongation by 4.5√A	Hardness, HV	Young's modulus, GPa	Type of fracture	Region
Sheet specimens							
1. Solution annealed at 1093 K for 1 h	910	1005	11.95	319-335	195	Ductile	···
2. Aged at 758 K for 3 h	1732	1885	6.37	530-560		Brittle	···
3. Aged at 758 K for 5 h	1760	1916	6.58	520-550		Brittle	···
4. Aged at 773 K for 5 h	1758	1910	6.75	520-540		Brittle	···
Welded specimens							
1. Solution Annealed at 1093 K for 1 h	925	1028	11.70	319-335	195	Ductile	Weld
2. Aged at 758 K for 3 h	1630	1770	6.0	520-540		Brittle	HAZ
3. Aged at 758 K for 5 h	1635	1773	5.6	520-540		Brittle	HAZ
4. Aged at 773 K for 5 h	1675	1790	6.8	520-550		Brittle	Weld
5. Aged at 793 K for 5 h	1595	1758	5.5	520-530		Brittle	HAZ
6. Aged at 823 K for 5 h	1458	1585	7.0	485-500		Brittle	HAZ

Solution annealing of sheet specimens were carried out at 1093 K for 1 h and aging treatments at 758 and 773 K for 3 and 5 h in electric-resistance heating furnace whereas, welded specimens were aged at 758, 773, 793, and 823 K for 3 and 5 h at a heating rate of 373 K/h. All the specimens were air cooled to room temperature. Since, it has been reported by many researchers (Ref 6-8) that reversion of austenite and coalescence of precipitates occurs above 773 K, so most of the work was confined to aging temperature of 773 K.

Tensile tests were carried out on sheet and welded specimens of rectangular cross section of standard ASTM E8 sizes in solution annealed and aged condition. All tensile tests were performed on 250 kN universal testing machine at a load rate of 0.50 kN/s at room temperature. Percentage elongation in each specimen (sheet and welded) was precisely measured by electric resistance-type strain gauges and also by joining two fractured pieces.

Impact tests were carried out on charpy V-notch substandard specimens as per ASTM standard E-23 on Roell/Armsler impact testing machine using 300 J capacity hammer. Charpy impact test were done at room temperature on sheet and welded specimens in both solution annealed and aged conditions. For post-weld aged specimens, V-notch was machined in weld zone (fusion zone), light etched HAZ, and dark-etched HAZ. Fracture surfaces were observed under JEOL JSM6380A scanning electron microscope (SEM).

Macrostructural and microstructural studies were conducted in the as-weld and post-weld aged condition using optical microscope equipped with image analysis software and SEM (JEOL JSM6380A) equipped with energy dispersive x-ray (EDX). Both transverse face and capping face of the each specimen was grinded with fine emery paper up to 1200 grit paper and then polished using alumina powder of 5 μm followed by 0.5 μm and then final polishing to 0.05 microns using automatic polisher with control of speed, force, and time. Special care was taken to avoid excessive heating of required surface during grinding and polishing process. For optical microscopy, 10% nital and modified Fry's reagent (50 mL HCl + 25 mL HNO_3 + 1 g $CuCl_2$ + 150 mL H_2O) were used. ASTM grain size number of different zones of weld metal was also determined using image analysis software for comparison.

In addition to macro and microexaminations, microhardness measurements were also carried out on as-welded and post-weld aged specimens to characterize different regions. Microhardness measurements were carried out at 500 g load and 500× magnification. Averages of five hardness measurements are reported for each region. Macrohardness measurements were performed on vickers hardness tester using 100 kg load for 30 s. A layer of approximately 1 mm was removed from the sample surface by grinding and subsequently polished to avoid the possible influence of oxygen when specimens were characterized or tested. At least three measurements were taken for each specimen keeping in view the possibility of segregation or other defects.

3. Results

Tensile test and hardness results of sheet and welded specimens with various post-weld heat treatments are given in Table 2. The result of tensile properties is the average of at least three specimens for each test conditions (see Table 2). Average of five hardness measurements is reported for each specimen. The maximum scatter in the hardness measurements was found to be less than ±5 HV (see Table 2).

It was observed from Table 2 that the strength and % elongation after fracture of maraging steel sheet in solution annealed and in aged condition is quiet satisfactory and comparable with the data cited in literature for maraging steels (Ref 9, 10). Peak hardness of ~550 HV and strength ~1900 MPa was achieved in sheet specimens with reasonable ductility, i.e., 6.75% el after aging for 5 h at 773 K. However, the hardness and strength of the post-weld aged specimens was found decreased with some rise in ductility than the aged sheet

specimens. Somewhat similar observations were reported earlier elsewhere (Ref 10). Weld efficiency of approximately 93% was obtained. It was further observed that the strength and hardness decrease with the increase in the aging temperature above 773 K with some rise in ductility and is expected to be the result of either the overaging of intermetallic precipitates or reversion of austenite. In case of maraging steel weldments, reverted austenite is of more interest in raising ductility of welds (Ref 10). Except for weld specimens aged at 773 K for 5 h, all the post-weld aged specimens were fractured from HAZ in a brittle manner. Macrohardness values measured on sheet and welded specimens in solution annealed and aged conditions were also given in Table 2. The optimum mechanical properties were obtained after aging treatment of 5 h at 773 K.

Table 3 Results of V-notch charpy impact test on sheet and welded specimens in annealed and aged conditions

Treatment	Energy absorbed, J	Fracture surface
Sheet specimens		
Solution annealed at 1093 K for 1 h	30	Ductile
Aged at 773 K for 5 h	20	Partially ductile
Welded specimens		
Notch in weld (fusion) zone		
Solution annealed at 1093 K for 1 h	29	Ductile
Aged at 758 K for 3 h	8	Brittle
Aged at 773 K for 5 h	16	Brittle
Notch in light etched HAZ		
Aged at 758 K for 3 h	8	Brittle
Aged at 773 K for 5 h	10	Brittle
Notch in dark etched HAZ		
Aged at 758 K for 3 h	14	Brittle
Aged at 773 K for 5 h	16	Brittle

Table 3 shows the results of impact tests obtained on sheet and welded specimens with various heat treatments and notches in different regions of the weld joint. Two specimens for each heat treated condition were fractured and the average impact value (in joules) along with location of fracture is given.

From Table 3, it can be seen that the impact resistance of sheet specimens in annealed and aged conditions is higher than welded specimens and mode of fracture is also ductile rather than brittle as in the case of post-weld aged specimens. Table 3 also enlists the impact energies absorbed by the specimens with V-notch in different regions. It was observed that light-etched HAZ is brittle and less resistant to impact as compared to weld zone and dark-etched HAZ in all aged conditions due to higher hardness. Furthermore, weld specimens aged at 773 K for 5 h exhibit better impact properties as compared to specimens aged at 758 for 3 h. Impact resistance of weld joints can be improved by solution annealing at 1093 for 1 h prior to aging treatment. SEM fractographs of impact specimens aged at 773 K for 5 h with V-notch in different regions of weld joint are shown in Fig. 1.

Microstructures of maraging steel sheets in solution annealed (1093 K for 1 h) and aged (773 K for 5 h) condition after etching with 10% nital are shown in Fig. 2(a) and (b), respectively.

Microstructure of solution annealed and aged specimen shows the regular bcc lath martensite. However, slight change in appearance of aged structure from annealed is due to precipitation of intermetallic compounds (i.e., Ni_3Mo and/or Fe_2Mo)

After suitably preparing the as-welded specimens for macroexamination, specimens were etched in 10% nital to reveal different zones produced by four pass GTAW welding. Change in structures of multipass welded joint can be seen as

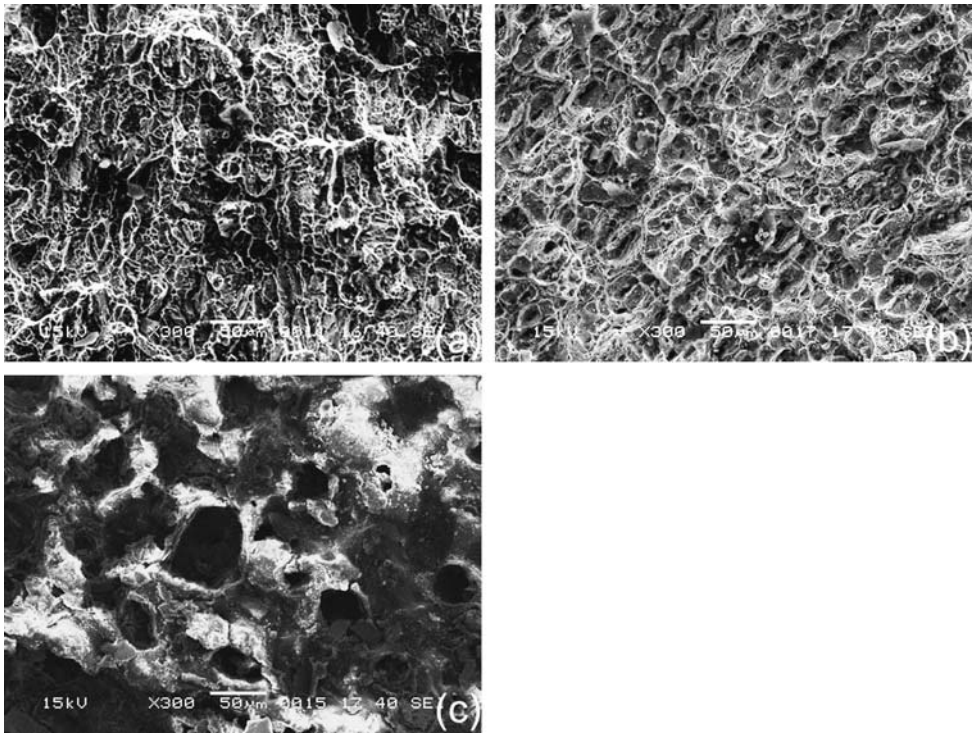

Fig. 1 SEM fractographs showing brittle transgranular fracture surface and dimples in (a) weld zone, (b) light-etched HAZ, and (c) dark-etched HAZ

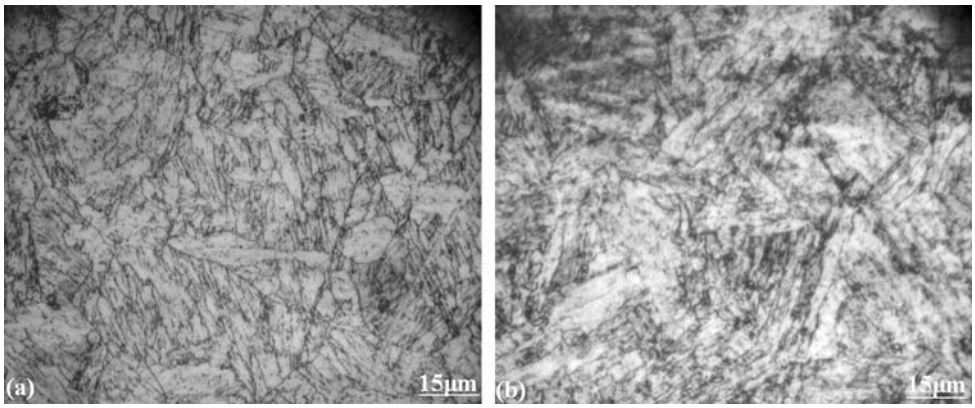

Fig. 2 Micrographs of maraging steel grade 250 sheets in (a) solution annealed and (b) aged condition

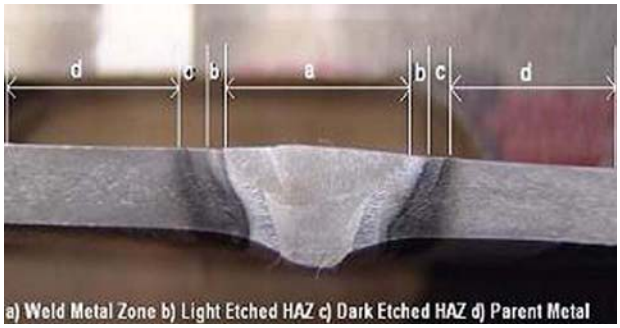

Fig. 3 Macrostructures produced in as-welded specimen

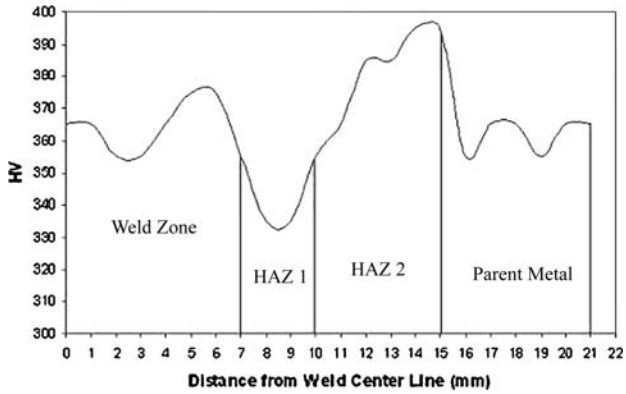

Fig. 4 Microhardness measurements taken in different zones of as-welded specimen

we move from weld pool to parent metal traverse across the weld joint. Similar to weld structures in other steels, weld joints of maraging steels also consist of three distinct regions that is the weld zone, the heat-affected zone (HAZ), and the parent metal. However, the HAZ in this case consists of two distinctly identified regions (b and c) that are light-etched HAZ 1 (zone b) and then narrow dark-etched HAZ 2 (zone c) as shown in Fig. 3.

Microhardness measurements across the transverse section of multipass as-welded specimen are shown in Fig. 4. Microhardness measurements also confirmed different zones in the weld joint.

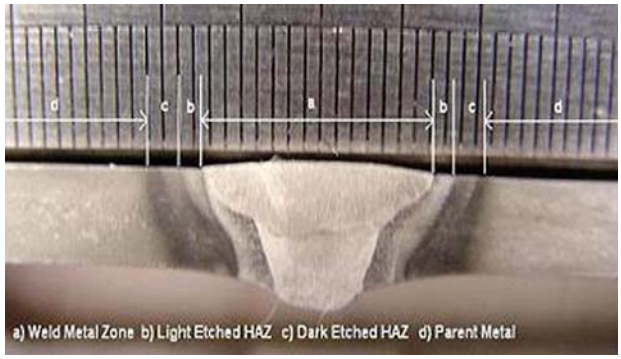

Fig. 5 Macrostructures produced in post-weld aged specimen

Figure 4 shows that as we move from weld center toward parent metal the hardness drops in light etched HAZ 1, whereas it increases in dark etched HAZ 2. This change in hardness was due to heat of welding. The dark-etched region was heated to aging temperature (773-873 K) and attained this hardness due to precipitation of intermetallic compounds.

Post-weld aged specimens were macro-etched in 10% ammonium persulphate solution to reveal different zones, as shown in Fig. 5. Macrostructures produced in welded + aged specimens are similar to the structures produced in as-welded specimen. However, there was difference in hardness values of HAZ of post-weld aged specimen from HAZ of as-welded specimen, as shown in Fig. 6. Microhardness measurements taken in different regions of post-weld aged specimens (aged at different temperatures for varying time periods) are given in Fig. 6.

Figure 6 illustrates that hardness in HAZ 1 raised after aging treatments, whereas hardness in HAZ 2 decreased. Since HAZ 2 of as-welded specimen was already aged by welding heat therefore aging the welded joint causes the overaging and softening of intermetallic precipitates in dark band. This causes little softening in HAZ 2 with some rise in hardness of HAZ 1. Microhardness values of solution annealed (at 1093 K for 1 h) and aged (at 773 K for 5 h) specimen in Fig. 6 showed that hardness slightly rises in HAZ 1 and then becomes almost uniform in HAZ 2 and parent metal. However, hardness of the weld joint became uniform after post-weld homogenizing (at 1373 for 8 h) and aging (773 K for 5 h) treatment.

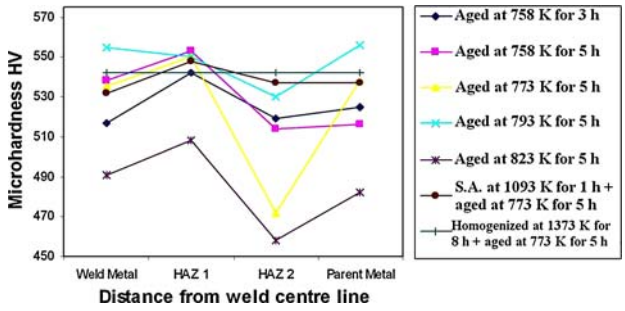

Fig. 6 Microhardness measurements taken in different zones of post-weld aged specimens, aged at varying temperatures and time periods

Microstructure of as-welded specimen was revealed by 10% nital as shown in Fig. 7. The principal microstructural change in the weld fusion zone is the transformation of austenite to martensite on cooling to room temperature. Contact between the weld metal and parent metal initially caused melting back of the adjacent parent metal and dilution of the filler metal, therefore structure of the weld metal reflects cast equiaxed structure as seen in Fig. 7(a). Weld zone mainly consists of cellular martensitic structure (Fig. 7a) whereas regions adjoining the fusion boundary exhibited a dendritic morphology (as seen in Fig. 8) with finer grain size (i.e., ASTM grain size no. 9) than in weld zone (ASTM grain size no. 8.25). The orientation of the grains in these zones changes from layer to layer depending upon thermal gradients. Weld zone becomes

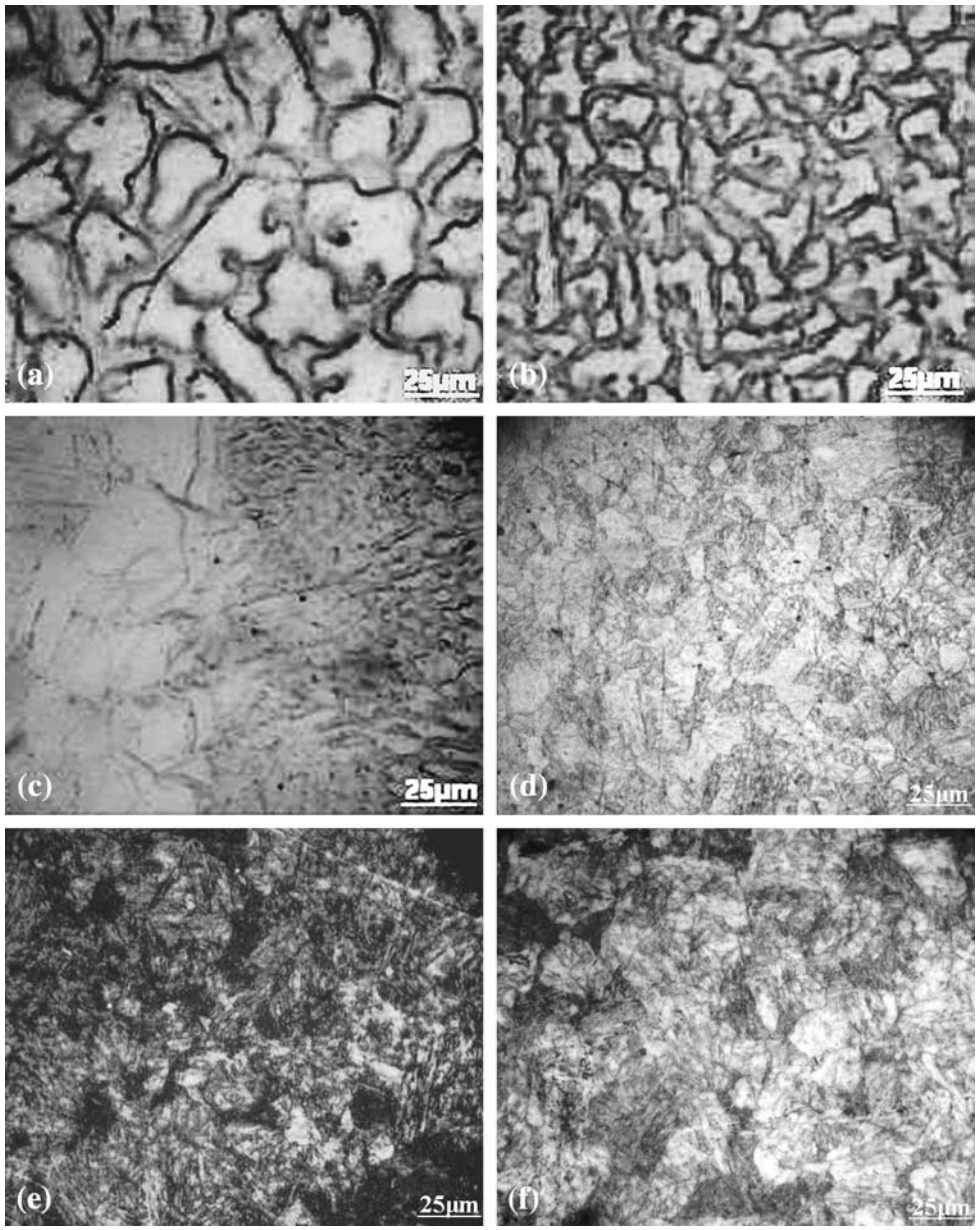

Fig. 7 Micrographs of different regions of as-welded specimen produced by multipass welding (a) weld zone-coarse grained, (b) weld zone-fine grained, (c) fusion boundary, (d) light-etched HAZ 1, (e) dark-etched HAZ 2, and (f) parent metal

Fig. 8 Micrograph of weld zone adjacent to fusion boundary showing cellular-dendritic morphology of grains

coarser due to thermal conditions produced during multipass welding. It was observed in Fig. 7(a) and (b) that the cell boundaries did not interfere with the martensite matrix rather the martensite blocks intersect them freely. The same microstructural aspect was also reported earlier (Ref 11). Adjacent to the fusion boundary is the light etched HAZ 1, which is affected very little by the etchant. It has bcc lath martensitic structure (Fig. 7d). Its structure is similar to that obtained in parent metal, except for a larger grain size in HAZ 1 (ASTM grain size no. 6.5-7).

Adjacent to the HAZ 1 lays narrow HAZ 2 which was heated to aging temperature (between 773 and 873 K); therefore, it etches black (Fig. 7e). It consists of martensite matrix with a fine dispersion of reverted austenite. This austenite is so small that it cannot be resolved by optical microscope, but was observed at higher magnification in SEM (Fig. 9e). Dark band of narrow size is desirable, since it is a weak region and plays a critical part in crack initiation. Width of dark band can be changed by varying the heat input and inter-pass temperature. Adjacent to the dark band region is the

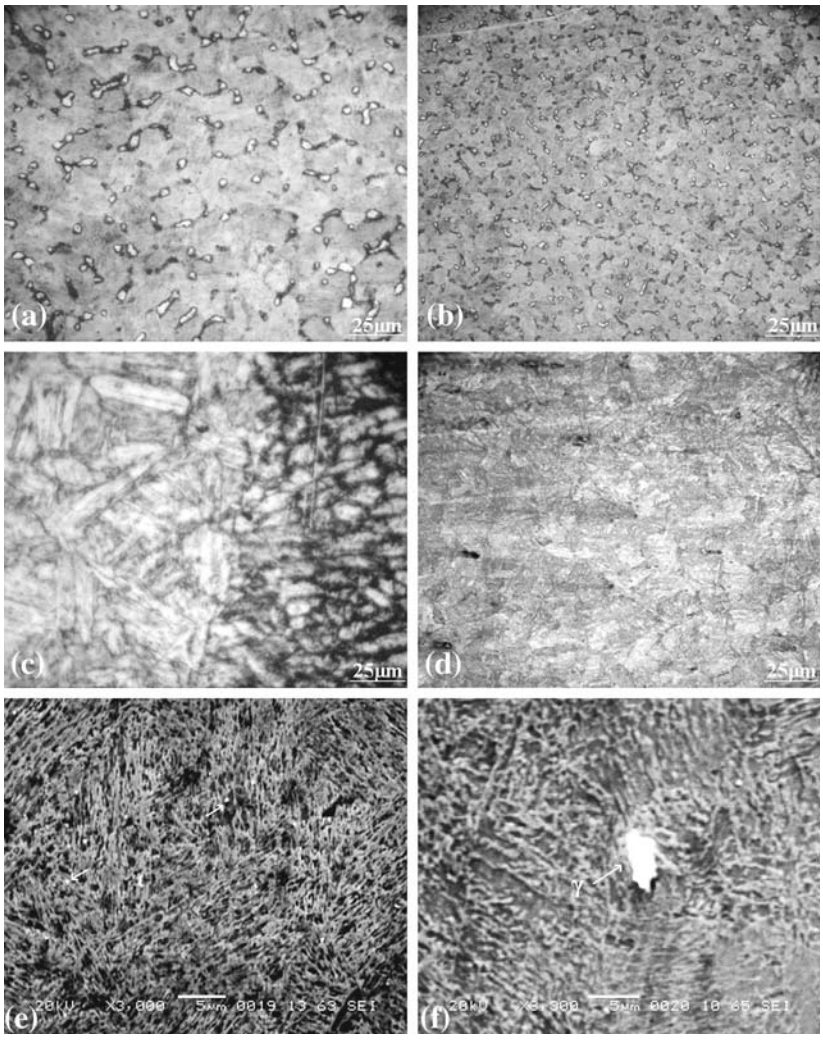

Fig. 9 Micrographs of different regions of welded specimen after aging at 773 K for 5 h (a) weld zone-coarse grained, (b) weld zone-fine grained, (c) fusion boundary, (d) light-etched HAZ 1, (e) SEM photo of dark-etched HAZ 2 (*arrow* indicates austenite), and (f) SEM photo of weld zone showing reverted austenite

Table 4 Average chemical composition of reverted austenite phase in aged weldments of maraging steel grade 250

Elements	Ni	Co	Mo	Ti	Fe
Wt.%	20	8.39	9.5	0.98	Balance

parent metal that is not exposed to high temperatures, so it has regular bcc martensitic structure (Fig. 7f). ASTM grain size number in parent metal region was found to be around 7.

Figure 9 shows microstructures produced in post-weld heat treated specimen that was aged at 773 K for 5 h (to peak hardness) and etched by modified Fry's reagent. A marked difference was observed in structures of weld + aged specimen from as-welded specimen. From a precipitate-free martensitic structure in the unaged condition, the structure was changed within few hours to a martensite containing finely dispersed precipitates of intermetallic compounds. Another interesting point observed was the presence of white pools (light etched) of reverted austenite surrounded by dark etched region in weld zone (fusion zone) of aged specimen, present on intersection points of cell boundaries as seen in Fig. 9(a). These austenite pools were not observed in weld zone of as-welded specimen shown in Fig. 7(a). Microstructures formed in other zones during post-weld aging are very similar to those produced in as-welded joints except reversion of large patchy pools of austenite on cell boundaries in aged condition (Fig. 9f). Chemical composition of reverted austenite phase (white pools) was measured by EDX spectrometry in order to confirm their existence, as shown in Table 4.

It was observed from Table 4 that %Ni in reverted austenite is approximately 20% as compared to 18% in martensite matrix, whereas Mo was found to segregate to an appreciable extent, i.e., from approx 5-9.5%. Furthermore, Ti was also found to segregate to some extent. The segregation of large amount of Mo was expected to be the result of dissolution of Mo-rich precipitates like Ni_3Mo forming lave Fe_2Mo precipitates (at higher temperature due to thermal cycling), thus enriching some regions in Ni content. These localized Ni-rich regions have lower A_s (austenite start) temperature and thus transformed to austenite on cooling.

Since it has been reported (Ref 12) that the amount of reverted austenite varied with post-weld aging time and temperature, therefore different aging treatments were examined to observe its affect on % vol. of reverted austenite. The aging treatments carried out were 758 K for 3 and 5 h, 773 K for 5 h, 793 K for 5 h, and 823 K for 5 h. Figure 10 shows changes in microstructure of weld zone after different aging treatments.

The amount of austenite thus formed after aging at different temperatures for varying time period was estimated using image analysis software and given in Fig. 11.

4. Discussion

From Table 2, it was observed that the weld efficiency of the weld seams in solution annealed condition and post-weld aged condition was about 92-93%. However, in welded specimens for tensile test it was observed that the fracture was initiated from HAZ. Increase in % elongation at fracture of welded joints aged at 773 K for 5 h was observed, and was expected as a result of the presence of significant amount of reverted austenite in the weld metal (shown in Fig. 9a and f). This increase in ductility of weld joint of maraging steel 250 due to presence of reverted austenite is in agreement with the data cited in Ref 10. Reverted austenite was not observed in as-welded specimens (Fig. 7a and b), it was formed in weld metal after aging of welds.

Generally, two different types of retained austenite formed in maraging steels: one obtained by the usual overaging process, and was found to be unstable at room temperature; the other, obtained due to thermal cycling in ferrite + austenite two phase region leading to the formation of micro-segregated zones, and was found to be thermally stable at room temperature. During multipass welding the lower layers heated to bi-phase temperature region and are aged, increasing the heterogeneity of the structure and properties of the weld seam. Also, precipitation during aging treatment is known to partition maraging steel into Ni-rich regions and Ni poor regions. It can be said that greater the precipitation, the more the partitioning (Ref 13). Redistribution of alloying elements enriches some region in Ni content. Since Ni-rich regions have a lower austenite start (As) temperature with martensite start (Ms) temperature also decreased down to below room temperature, so these regions start transforming to austenite first, thereby splitting the martensite to austenite. The reverted austenite pools thus formed are thermally stable at room temperature (even does not transform into martensite on cryogenic cooling in liquid nitrogen) and are expected to form in regions where alloying elements have segregated during multipass welding. The presence of larger amount of Ni than normal in reverted austenite of maraging steels was also confirmed earlier (Ref 14). Mo and Ti are the most expected one to segregate as confirmed by EDX analysis in Table 4.

Figure 9 shows that reverted austenite decorates the cell boundaries of the weld zone (fusion zone) and there was no appreciable change in microstructures of weld zone aged at different temperatures for different times. However, the amount of reverted austenite increased with the rise in aging temperature (as shown in Fig. 10). Amount of austenite was not affected significantly by time of aging at any particular temperature. The least amount of reverted austenite was detected after aging at 758 K with subsequent decrease in hardness due to less amount of precipitation. The aging treatment at 793 K was found to produce a greatest degree of austenite reversion in the weld metal. In Fig. 10(e), it was interesting to observe that after aging at 823 K for 5 h the % vol. of reverted austenite in weld zone reduced and cell boundaries were also not present which were observed at lower aging temperatures. However, hardness obtained after aging at 823 K for 5 h was also lowered, i.e. 485 HV and thought to be the result of overaging of intermetallic precipitates at higher aging temperature. It was thought that the decrease in the % of reverted austenite at 823 K was due to less Ni content present in it, which causes some % of austenite to retransform to martensite on cooling to room temperature. Austenite reverted at higher temperatures contains less nickel; therefore, the higher the temperature of aging, the austenite is less rich in nickel and its stability decreases. The amount and stability of austenite formed in weld zone is thus controlled by adjusting aging temperature and time.

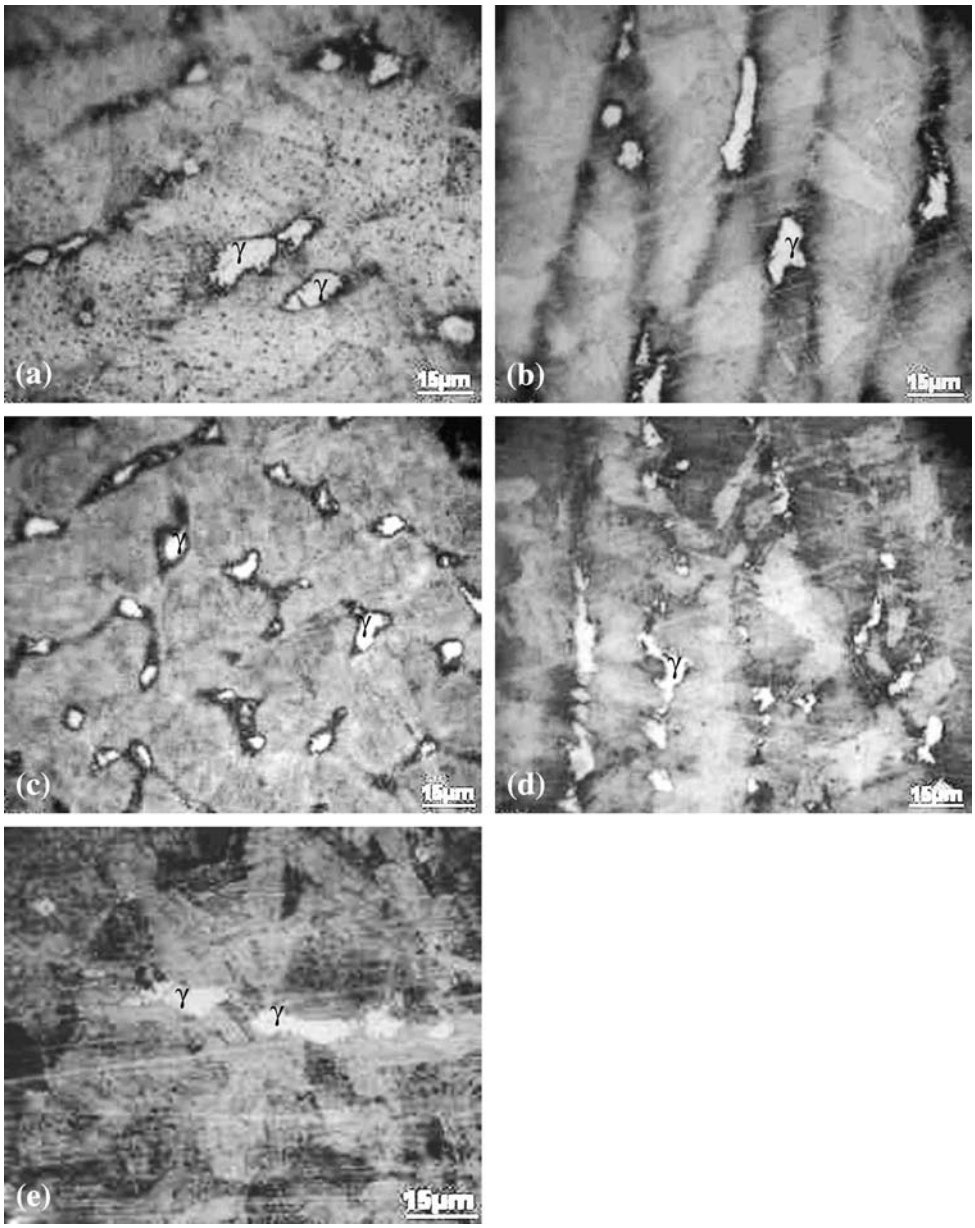

Fig. 10 Micrographs of weld zone after aging at (a) 758 K for 3 h, (b) 758 K for 5 h, (c) 773 K for 5 h, (d) 793 K for 5 h, and (e) 823 K for 5 h

It has been reported by many researchers in earlier studies that the austenite phase reduces strength (since it is a soft phase as compared to martensite), but it is interesting to see that in this investigation, the austenite formed due to thermal cycling caused by multipass welding does not decreases the strength to an appreciable amount, rather it increases the ductility. Same results were reported earlier (Ref 15) that increasing the amount of retained austenite (not more than 30%) in maraging steels leads to an increase in ductility without significantly reducing strength.

Although, austenite pools in welds of maraging steel are tough but the opinion has also been expressed that reverted austenite may even be detrimental to toughness; it has been argued that under load, deformation is concentrated in the softer austenite, which therefore reaches its critical strain for fracture at an early stage (Ref 11). Hence it is desirable to limit the amount of austenite in weld zone to below 15%. Since the reversion of austenite is mainly due to segregation of alloying elements during welding with subsequent formation of Ni-rich regions during aging, therefore, to reduce the segregation solution annealing at 1093 K for 1 h was carried out followed by aging at 773 K for 5 h. Figure 12(a) showed that austenite decorates the cell boundaries. There was no significant effect of solution annealing prior to aging on austenite; austenite remains stable. Solution annealing did not eliminate the segregation completely.

To completely remove the segregation (which accelerates at high temperatures and longer times due to high diffusion rates), homogenizing was carried out at 1373 K for 8 h with subsequent aging at 773 K for 5 h. The effect of high temperature treatment on weld zone is shown in Fig. 12(b).

In the absence of homogenizing treatment, reversion of austenite was observed as in Fig. 12(a), but after homogenizing the weld seam, the cellular structure, which is a common feature of welded maraging steel, is no longer visible as shown in Fig. 12(b). This demonstrates that solution annealing did not reduce the reversion of austenite, only homogenizing at high temperatures can completely eliminate the segregation and produce massive-type of martensite which is free of austenite. However, homogenizing at high temperatures produces coarser grain (ASTM grain size no. 6-6.5) due to recrystallization and grain growth. Hardness after homogenizing + aging at 773 K for 5 h also decreased down to 520 HV. It was expected that by reducing the time of homogenization the same martensitic structure will be produced without impairing the hardness. To verify this, homogenization was carried out at 1373 K for only 10 min with subsequent aging at 773 K for 5 h. Microhardness was also measurement for comparison.

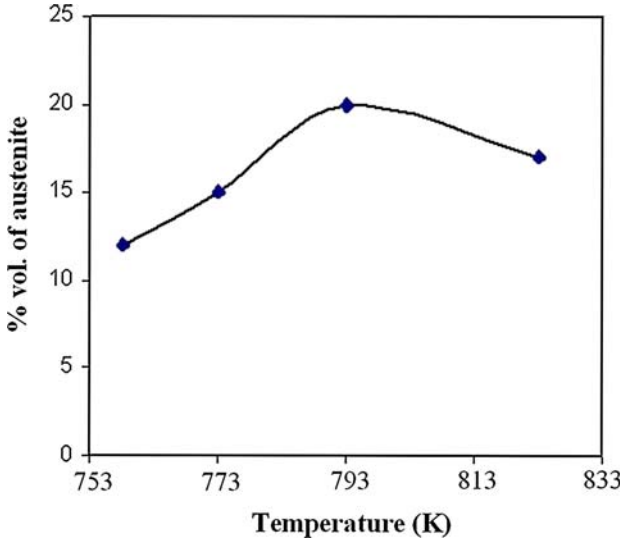

Fig. 11 % Volume of reverted austenite as a function of aging temperature (as calculated by optical microscopy)

It was interesting to see that heating the structure to higher temperature (1373 K for 10 min) leads to complete elimination of chemical heterogeneity and the weld zone now consists of lath-type martensite (Fig 13a). Furthermore, after aging this homogenized structure at 773 K for 5 h, only aged martensite exists with no visible reverted austenite (Fig 13b). Also, hardness was uniform throughout the structure and found to have slightly increased in the range of 540-550 HV whereas the ASTM grain size number was now 6.5-7.0 against previous measured grain size number of 6-6.5. Increasing the time of homogenization up to 8 h, had no apparent effect on microstructure; however, hardness and ASTM grain size number was

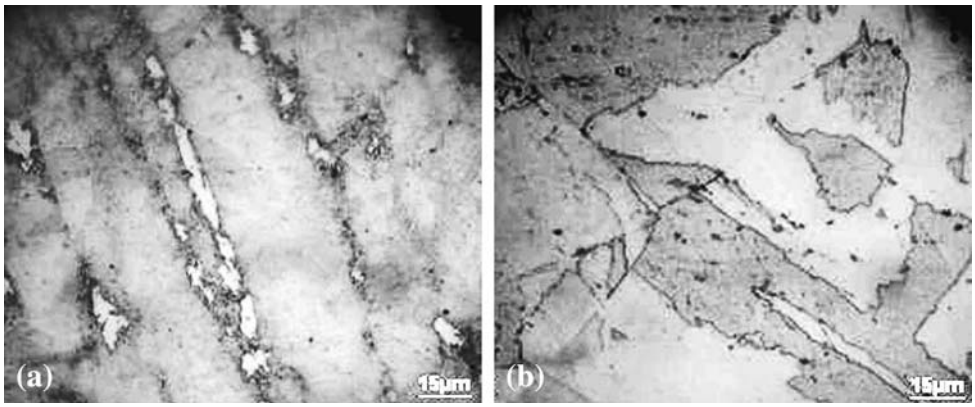

Fig. 12 Micrographs of weld zone after (a) solution annealing at 1093 K for 1 h and (b) homogenizing at 1373 K for 8 h followed by aging at 773 K for 5 h

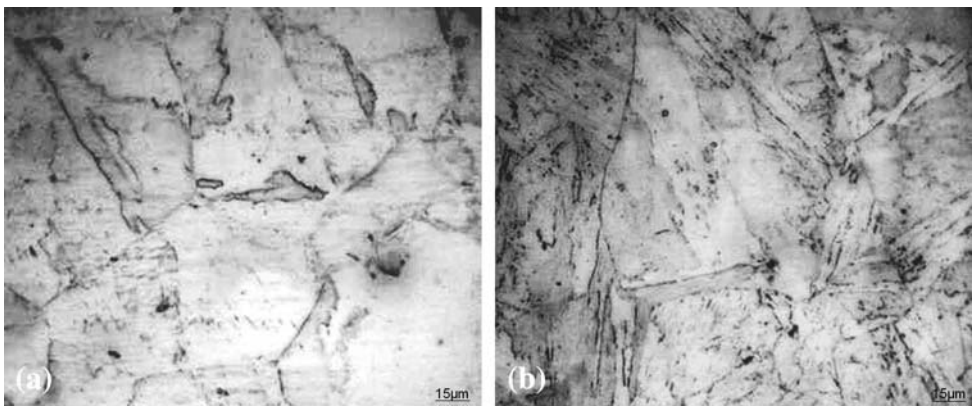

Fig. 13 Micrographs of weld zone after (a) homogenizing at 1373 K for 10 min and (b) aging the homogenized structure at 773 K for 5 h

found to have slightly increased. This change in hardness and grain size by varying homogenizing time requires further detailed investigation.

It was thus observed that the reversion of austenite in weld zone of post-weld aged specimens was primarily a result of segregation. In this regard, Mo is the most contributing element. Aging at high temperatures causes dissolution of Ni_3Mo precipitates with subsequent formation of Fe_2Mo precipitates. This results in increase in Ni content of matrix which leads to austenite reversion. However, homogenizing the structure at 1373 K completely removes the chemical heterogeneity in the weld seams and on subsequent aging treatment; microstructure consists of austenite-free lath martensite.

5. Conclusion

The experimental data obtained lead us to conclude that:

1. Optimum set of mechanical properties in welded joints were obtained after aging at 758 K for 5 h.
2. Macrostructure of multipass weld joints consists of different regions: weld zone, fusion boundary, light etched zone, dark-etched zone, and parent metal. Microhardness survey also confirmed existence of these zones.
3. In weld joints, made with filler wire of similar composition, significant amount of stable reverted austenite was observed after aging at intersection points of cell boundaries. The maximum amount of reverted austenite calculated in weld zone was about 19% after aging at 793 K for 5 h.
4. Presence of stable reverted austenite after aging treatment was due to extensive segregation of alloying elements (mostly Mo) due to thermal cycling cause by multipass welding which encourages local enrichment of matrix in Ni content. Highly enriched austenite thus formed did not undergo austenite $\rightarrow$ martensite transformation upon subsequent cooling; even cooling down to liquid nitrogen temperature.
5. Since Mo and Ti are the most expected elements for segregation, therefore properties of the weld seams can be improved by using welding wire of slightly lower Mo content and slightly higher Co content (Ref 10, 16, 17).
6. It was found that solution annealing at 1093 K for 1 h was not sufficient for complete homogenization and therefore reverted austenite was still observed after aging. However, homogenizing at 1373 K eliminates the heterogeneity completely with subsequent formation of massive-type of martensite free of reverted austenite after aging treatment. However, the effect of ''time for homogenization'' on structural-sensitive properties will require a detailed further investigation.

Acknowledgments

This research was carried out in the Materials Research and Testing Laboratory of Pakistan Space and Upper Atmosphere Research Commission (SUPARCO). The authors wish to thank Mr. Badar-ul-Hasan for his technical assistance in experimental work, Mr. Muhammad Saraf (Deputy Chief Manager) and Dr. Sajid Mirza (Senior Chief Manager) for their valuable guidance in this work, and Mr. Raza Hussain (Chairman) for the provision of facilities and their suggestions throughout the project.

References

1. V.K. Vasudevan, S.J. Kim, and C. Marvin Wayman, Precipitation Reactions and Strengthening Behavior in 18 Wt Pct Nickel Maraging Steels, *Metall. Trans. A*, 1990, **21A**, p 2655–2668
2. M. Ahmed, K. Hasnain, I. Nasim, and H. Ayub, Magnetic Properties of Maraging steels in Relation to Nickel Concentration, *Metall. Mater. Trans. A*, 1995, **26A**, p 1869–1876
3. V. E. Laz'ko, Regular Changes in the Strength of Maraging Steels Upon Complex Alloying with Cobalt, Nickel, and Molybdenum, Translated from Metallovedenie i Termicheskaya Obrabotka Metallov, Vol. 2, 2001, p 25–28
4. G.P. Miller and W.L Mitchell, Structure and Hardening Mechanisms of 18% Nickel-Cobalt-Molybdenum Maraging Steels, *J. Iron Steel Int.*, 1965, **203**, p 899–904
5. F.H. Lang and N. Kenyon, Welding of Maraging Steel, *WRC Bulletin* **159**
6. M.D. Perkas, High-Strength Maraging Steels, Translated from Metallovedenie i Termicheskaya Obrabotka Metallov, vol. 6, 1968
7. A.F. Edneral and M.D. Perkas, Structural Changes during Aging of Fe-Ni-Mo Alloys, *Fiz. Metal. Metalloved.*, 1970, **28**(5), p 862
8. A.F. Edneral and M.D. Perkas, The Aging of Martensite of N18K9M5T Steel, Translated from Metallovedenie i Termicheskaya Obrabotka Metallov, vol. 6, 1968, p 18–19
9. Nickel Development Institute, 18% Nickel Maraging Steels: Engineering Properties, Publication No. 4419, 1976, p 6–7
10. C.R. Shamantha, R. Narayanan, K.J.L. Iyer, V.M. Radhakrishnan, S.K. Seshadri, S. Sundararajan, and S. Sundaresan, Tensile Properties and Fracture Toughness of 18Ni (250 Grade) Maraging Steel Weldments, *Sci. Technol. Weld. Join.*, 2000, **5**(5), p 329–337
11. C.R. Shamantha, R. Narayanan, K.J.L. Iyer, V.M. Radhakrishnan, S.K. Seshadri, S. Sundararajan, and S. Sundaresan, Microstructural Changes During Welding and Subsequent Heat Treatment of 18Ni (250-grade) Maraging Steel, *Mater. Sci. Eng. A*, 2000, **287**, p 43–51
12. D. T. Peters and C. R. Cupp, The Kinetics of Aging Reactions in 18 Pct Ni Maraging Steels, *Trans. Metall. Soc. AIME*, 1966, **236**, p 1420–1429
13. M.M. Shtrikman, I.P. Kapranova, and E.T. Romanova, Structure and Properties of Welds in Maraging Steel N18K9M5T, Translated from Metallovedenie i Termicheskaya Obrabotka Metallov, vol. 10, 1972, p 18–22
14. N.F. Lashko, L.N. Belyakov, L.V. Zaslavskaya, and L.I. Polyanieheva, Phase Composition of Maraging Steels, Translated from Metallovedenie i Termicheskaya Obrabotka Metallov, 1969, 10, p 26–29
15. O.V. Abramov, A.I. Il'in, and V.M. Kardonskii, Effect of Heat Treatment on the Mechanical Properties of Maraging Steel, Translated from Metallovedenie i Termicheskaya Obrabotka Metallov, vol .4, 1983, p 43–46
16. J.M. Vehida, Investigation of Experimental Filler Alloys for 18% Ni Maraging Steel (300), The Boeing Company Report D2-236901-1, 1965
17. D.A. Corrigan, Gas-Shielded Arc Welding of 18% Ni Maraging Steel, *Weld. J.*, 1964, **43**(Research Suppl), p 289–294